The EMBO Journal Vol.16 No.24 pp.7219–7230, 1997

The 1.25 Å crystal structure of sepiapterin reductase reveals its binding mode to pterins and brain neurotransmitters

Günter Auerbach[1], Anja Herrmann[2], Markus Gütlich[2], Markus Fischer[2], Uwe Jacob, Adelbert Bacher[2] and Robert Huber

Max-Planck-Institut für Biochemie, Abt. Strukturforschung, Am Klopferspitz 18a, D-82152 Martinsried, Germany and [2]Technische Universität München, Institut für Organische Chemie und Biochemie, Lichtenbergstrasse 4, 85748 Garching, Germany

[1]Corresponding author
e-mail: auerbach@biochem.mpg.de

Sepiapterin reductase catalyses the last steps in the biosynthesis of tetrahydrobiopterin, the essential co-factor of aromatic amino acid hydroxylases and nitric oxide synthases. We have determined the crystal structure of mouse sepiapterin reductase by multiple isomorphous replacement at a resolution of 1.25 Å in its ternary complex with oxaloacetate and NADP. The homodimeric structure reveals a single-domain α/β-fold with a central four-helix bundle connecting two seven-stranded parallel β-sheets, each sandwiched between two arrays of three helices. Ternary complexes with the substrate sepiapterin or the product tetrahydrobiopterin were studied. Each subunit contains a specific aspartate anchor (Asp258) for pterin-substrates, which positions the substrate side chain C1′-carbonyl group near Tyr171 OH and NADP C4′N. The catalytic mechanism of SR appears to consist of a NADPH-dependent proton transfer from Tyr171 to the substrate C1′ and C2′ carbonyl functions accompanied by stereospecific side chain isomerization. Complex structures with the inhibitor *N*-acetyl serotonin show the indoleamine bound such that both reductase and isomerase activity for pterins is inhibited, but reaction with a variety of carbonyl compounds is possible. The complex structure with *N*-acetyl serotonin suggests the possibility for a highly specific feedback regulatory mechanism between the formation of indoleamines and pteridines *in vivo*.

Keywords: crystal structure/*N*-acetyl serotonin/SDR family/sepiapterin reductase/tetrahydrobiopterin

Introduction

Tetrahydrobiopterin (BH_4) is a multifunctional cofactor for phenylalanine, tyrosine and tryptophan hydroxylases, which catalyse the initial steps in phenylalanine degradation in the liver, and are the rate-limiting steps in the biosynthesis of the neurotransmitters, catecholamines and indoleamines in the brain.

A function to promote release of dopamine, serotonin and noradrenaline from the striatal and cortical nerve terminals has also been proposed for BH_4 (Mataga *et al.*, 1991). Serotonin (5-hydroxytryptamine; 5-HT) and its derivatives are neurotransmitters present in brain or pituitary gland, regulating a great number of physiological mechanisms such as sleep, appetite, thermoregulation, control of pituitary secretions and behaviour (McGeer *et al.*, 1987). BH_4 has furthermore an essential role in the biosynthesis of nitric oxide (NO) (Lowenstein and Snyder, 1992; Marletta, 1994) as an allosteric activator of nitric oxide synthase (NOS) and seems to be necessary for catalytic turnover involving a redox-function of the co-factor (Hemmens and Mayer, 1996). Recently, it was shown that an increase in BH_4 biosynthesis in a pancreatic B-cell line (INS-1) is followed by enhanced NO production and subsequently, inhibition of insulin secretion (Laffranchi *et al.*, 1997). BH_4 regulates human melanogenesis by forming a stable complex with the α-melanocyte-stimulating hormone (Schallreuter *et al.*, 1994). Finally, BH_4 is known as an essential co-factor for alkylglyceryl monooxygenases (Pfleger *et al.*, 1967).

Reduced levels of BH_4 in the brain and cerebrospinal fluid are associated with several neuropsychiatric diseases such as Parkinson's disease, Alzheimer's disease, depression and dystonia (Lovenberg *et al.*, 1979; Curtius *et al.*, 1983). In atypical phenylketonuria (PKU), BH_4 deficiency results in neurological disorders as a result of decreased biosynthesis of brain catecholamines and serotonin. BH_4 is involved in proliferation and growth regulation of erythroid cells. Partial depletion of BH_4 in a murine erythroleukaemia cell line caused inhibition of cell growth (Tanaka *et al.*, 1989).

The complex organic chemistry involved in *de novo* formation of BH_4 from GTP is catalysed by only three enzymes. The first committed step is catalysed by GTP cyclohydrolase I (EC 3.5.4.16; CYH) conducive to the formation of dihydroneopterin triphosphate. This intermediate is transformed to 6-pyruvoyl tetrahydropterin (6-PPH_4) by 6-pyruvoyl tetrahydropterin synthase (EC 4.6.1.10; PTPS, PPH_4S). Finally, sepiapterin reductase (EC 1.1.1.153; SR) reduces this diketo compound in an NADPH-dependent step to BH_4. Recently, the crystal structures of *Escherichia coli* CYH (Nar *et al.*, 1995a,b) and rat liver PTPS (Nar *et al.*, 1994; Bürgisser *et al.*, 1995) were solved by isomorphous replacement techniques (Auerbach and Nar, 1997). The crystal structure of mouse sepiapterin reductase (mSR) completes the structural analysis of all three enzymes involved in the BH_4 pathway (Figure 1). The biosynthetic pathway of BH_4 includes minimally these three enzymes; the participation of a fourth enzyme, aldose reductase, is suggested but still controversial. However, it was shown that aldose reductase is not important for BH_4 biosynthesis in liver (Milstien and Kaufman, 1989). Besides the *de novo* biosynthesis of BH_4, SR is also known to be involved in the pterin salvage pathway catalysing the conversion of sepiapterin

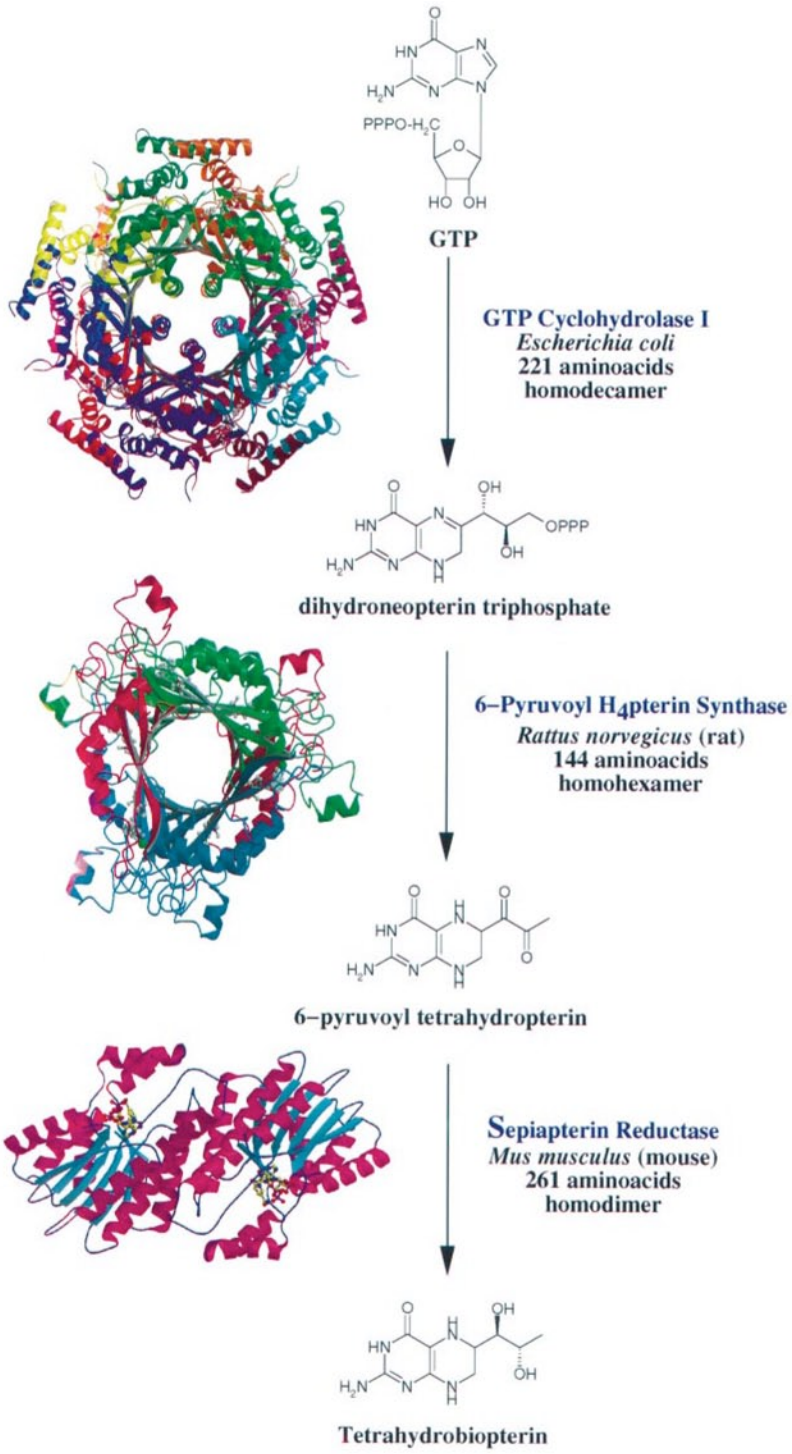

Fig. 1. The complete pathway of the *de novo* biosynthesis of BH_4. The cofactor BH_4 is synthesized by only three enzymes, namely CYH, PTPS and SR. The crystal structure of *E.coli* CYH was recently solved by single isomorphous replacement and averaging techniques. The enzyme complex, a decamer consisting of a pentamer of tightly associated dimers, has perfect D_5 symmetry and is doughnut-shaped with dimensions of 65×100 Å. The MIR-solved crystal structure of rat PTPS shows a hexameric enzyme composed of a dimer of trimers with D_3 symmetry. Each trimer forms a 12-stranded antiparallel β-barrel, enclosing a basic pore with 6–12 Å diameter. The crystal structure of mSR completes the structural analysis of all three enzymes involved in BH_4 biosynthesis, providing the essential information for the interpretation of the complex biochemical regulation of this pathway.

to dihydrobiopterin (BH_2) which is transformed by dihydrofolate reductase to BH_4 (Nichol *et al.*, 1983). Furthermore, a regeneration system for the cofactor is known involving pterin-4a-carbinolamine dehydratase (PCD) (Endrizzi *et al.*, 1995; Ficner *et al.*, 1995) and dihydropteridine reductase (DHPR) (Varughese *et al.*, 1992).

The full complement of the three BH_4-biosynthesizing enzymes can be found in significant amounts in many tissues of various species (Smith and Nichol, 1984). The richest sources of SR are erythrocytes, liver and brain. Katoh and co-workers (1982) have obtained evidence for a regulation mechanism of the BH_4 pathway by feedback

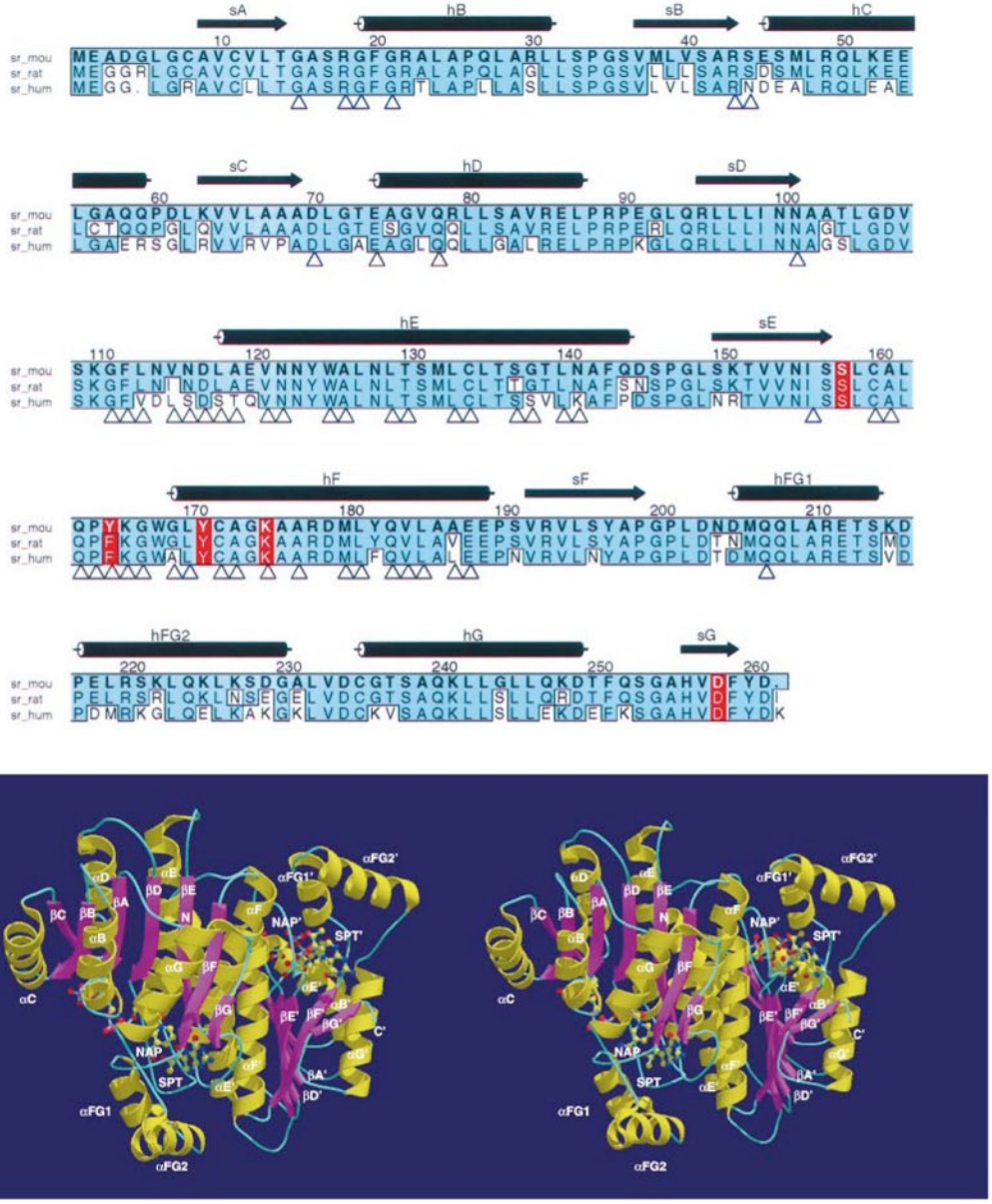

Fig. 2. Structure of mSR. (**A**) Primary structure of mSR. The sequence alignment of mSR with the rat and human enzyme reveals a weighted sequence similarity of 94% and 88%. Residues involved in cofactor binding are marked with a blue, residues involved in subunit interactions with a black triangle. Central residues for substrate binding, catalysis or inhibition are red inverted. The sequence numbering and secondary structure assignment is according to mSR sequence. (**B**) Stereo view of the quaternary structure of mSR. The 56 kDa dimer shows two parallel β-strands in anti-parallel orientation enclosing a four-helix bundle forming the subunit interactions. The substrate sepiapterin (SPT) and the cofactor NADP/NADPH (NAP) bind from opposite sides to the enzyme. The secondary structure elements and ligands are labelled, the components of the second monomer are marked with an apostrophe.

inhibition of the activity of SR in rat brain by a catecholamine and an indoleamine.

SRs from mouse, rat and human origin have been cloned and sequenced (Citron *et al.*, 1990; Ichinose *et al.*, 1991; Ota *et al.*, 1995) revealing a sequence identity of the mouse SR with rat and human enzymes of 88% and 74% (94% and 88% sequence similarity) (Figure 2A).

Here we describe a crystallographic structure analysis of mouse SR. All structures are complexes with the natural cofactor NADP, which was added during purification and crystallization. Surprisingly, recombinantly expressed protein contained oxaloacetate bound to the active site. The ternary complex structure of mouse SR with NADP and oxaloacetate was refined to a resolution of 1.25 Å. In order to investigate the catalytic mechanism of the enzyme, ternary complex structures either with the substrate, sepiapterin, or the product, tetrahydrobiopterin, have been analysed. Inhibitory complex structures were determined as quaternary complex with *N*-acetyl serotonin (NAS) and oxaloacetate (OAA), and as ternary complex structures with either NAS or noradrenaline.

Results and discussion

Overall structure of the SR

SR is a homodimer with 261 amino acids per monomer, each forming a single domain α/β-structure. A seven-stranded parallel β-sheet in the centre of the molecule is

sandwiched by two arrays of three α-helices (αC, αB, αG and αD, αE, αF). Six strands of them constitute a classical dinucleotide-binding motif (Rossmann *et al.*, 1975) composed of βαβ units (Figure 2B). The association of two SR monomers to a dimer leads to the formation of a four-helix bundle by helices αE and αF of each monomer, stabilized by numerous hydrogen bonds and two charged interactions involving Asn116 and Asn141

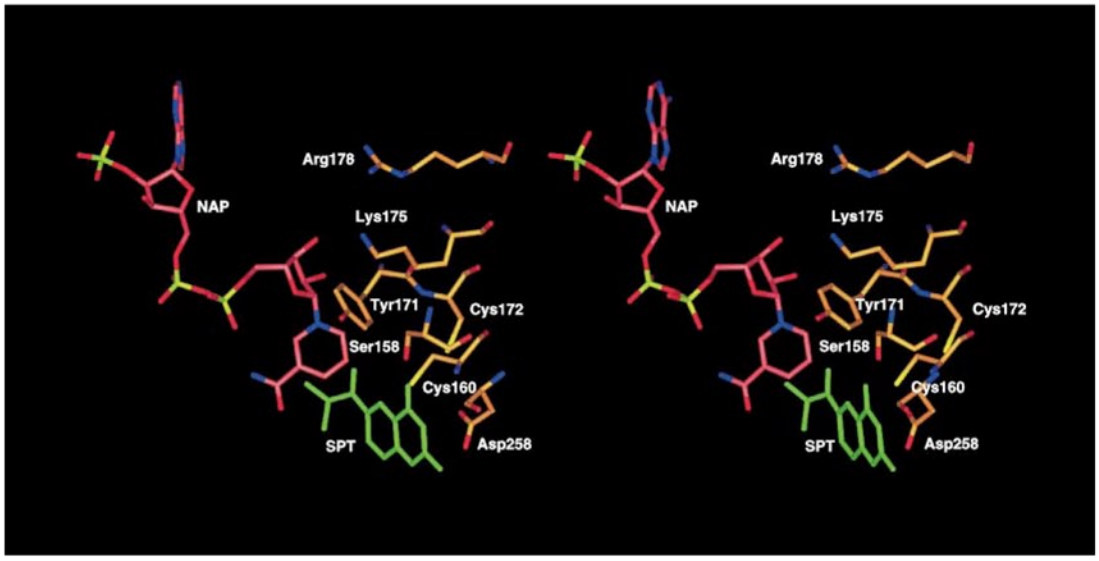

Fig. 3. Active site of mSR in complex with substrate sepiapterin (SPT) and cofactor NADP (NAP). Anchoring of sepiapterin with its purine moiety to Asp258 positions its C1′ carbonyl function in direct proximity to NADP and Tyr171, clearly indicating the latter as the central catalytic site for hydrogen transfer to the carbonyl function of the substrate.

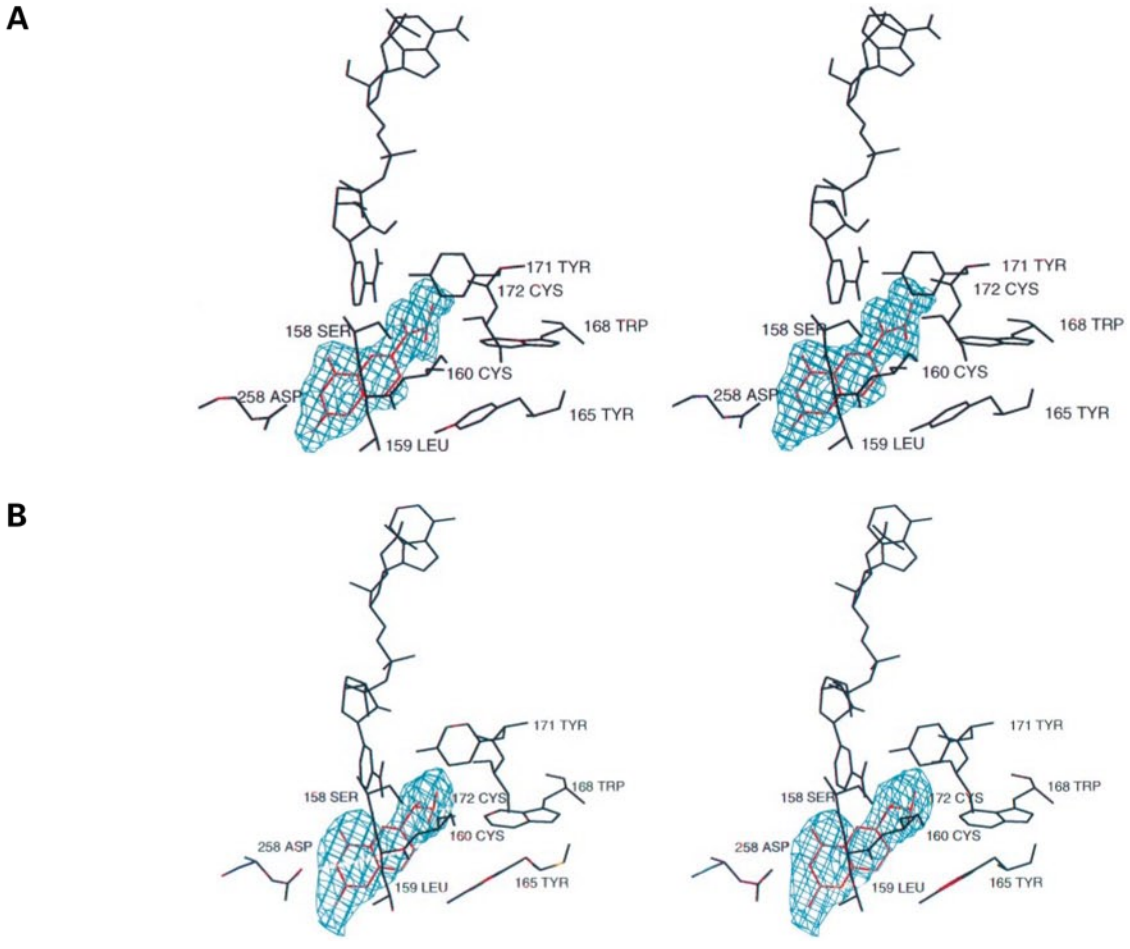

from each monomer. Exceptionally, the two parallel β-sheets of the dimer are in an anti-parallel orientation enclosing an angle of 90°. The two substrate pockets are opened to the same side of the molecule, each formed by elongation of the three loops between strand βD and helix αE, between βE and αF, and between βF and αG. The latter insertion contains two additional helices αFG1 and αFG2 (Figure 2).

From both amino acid sequence and three-dimensional structure, SR can be unequivocally assigned to the family of short-chain dehydrogenases/reductases (SDR). Although sequence comparison of these enzymes show sequence identities between 12% and 35% and their substrates are very different, they share a common tertiary structure. They all use either NAD(H) or NADP(H) as the cofactor and contain a strictly conserved Tyr-X-X-X-Lys sequence motif (Ghosh *et al.*, 1994).

Active site for reductase and isomerase activity

The presence of the nicotinamide ring of the bound cofactor NADP already indicates the location of the active site of SR, which is situated at the C-terminal end of the β-strands. The acceptor site for the substrate contains a 15 Å-deep pocket that is ideally suited to receive pterin and small carbonyl substrates. The active site cavity is formed by the hydrophobic residues Leu105, Leu159, Tyr165, Trp168, Tyr171, Met206 and Cys160. The crystal structure of SR in ternary complex with NADP and the substrate, sepiapterin, clearly shows the pterin substrate positioned in the active site anchored with its guanidino moiety to Asp258. This positions the pterin moiety with its side chain C1′-carbonyl function in direct proximity to Tyr171 OH and NADP C4′N. The crystal structures clearly show Tyr171 as the central active site residue in an orientation for optimal proton transfer to the carbonyl functional groups of the substrate. Furthermore, the nicotinamide group is co-planar with the side-chain carbon atoms for optimal hydride transfer to the carbonyl group (Figure 3). The electron density at the C2′-position in the ternary complex of SR with sepiapterin and NADP appears planar, thus indicating that sepiapterin is oxidized to the diketo compound in the soaked crystals (Figure 4A). The crystal structure of the ternary complex of the enzyme with NADPH and BH_4, the product of the catalysed reaction, confirms this orientation of the side chain also for the bound product (Figure 4B).

Three residues can be regarded as a central feature in the active site of SR for both reductase and isomerase activity. The two basic residues Lys175 and Arg178 may facilitate the proton transfer from the hydroxyl function

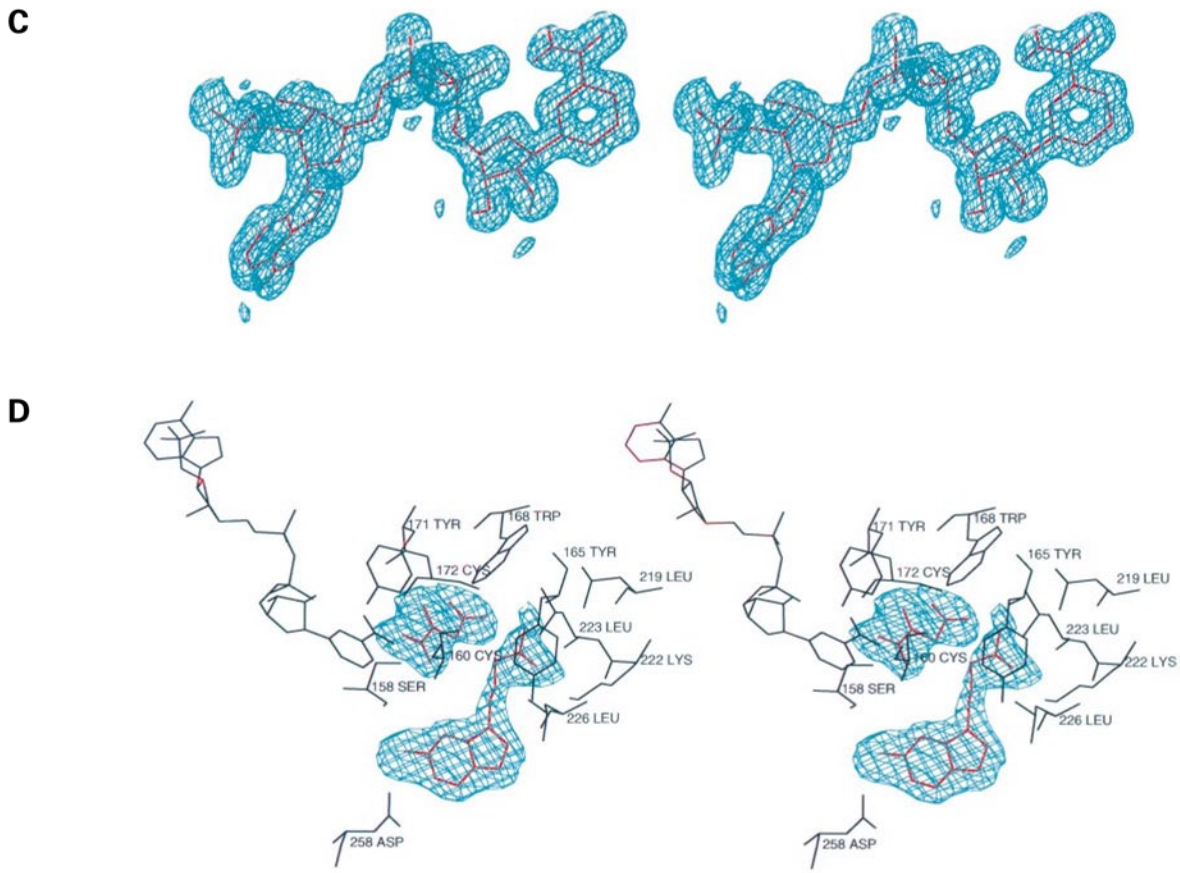

Fig. 4. Electron densities for the substrate sepiapterin (SPT), the product tetrahydrobiopterin (BH_4), the cofactor NADP, and the inhibitors *N*-acetyl serotonin (NAS) and oxaloacetate (OAA). (**A**) Stereo diagram showing the substrate sepiapterin in the enzyme-bound conformation placed in its 3σ contoured F_o–F_c density refined to 1.95 Å resolution and (**B**) the product tetrahydrobiopterin refined to 2.6 Å resolution. (**C**) Stereo view of the cofactor NADP placed in its 1 σ contoured $2F_o$–F_c density refined to 1.25 Å resolution. (**D**) Stereo view of the quaternary complex structure of SR with the two inhibitors OAA and NAS. NAS, anchored by Asp258, is a specific competitive inhibitor only for pterin substrates, while OAA bound to Tyr171 is probably an inhibitor for pterin- and non-pterin carbonyl compounds.

of Tyr171 to the substrate's carbonyl oxygen by stabilizing the resulting tyrosinate. The guanidinium group of Arg178 is in hydrogen bond distance to the side-chain amide groups of the three Asn residues, Asn100, Asn128 and Asn155, which are conserved at least within SR, carbonyl reductase, and *Drosophila* alcohol dehydrogenase.

From the crystal structure, a central role can also be proposed for residue Ser158, which is located in hydrogen bond distance to the substrate N5 atom and the C1′-side chain oxygen. Ser158 is presumably involved in stabilizing the position of the substrate, according to results from 7α-hydroxy steroid dehydrogenase (HSDH), mouse lung carbonyl reductase (MLCR) (Tanaka *et al.*, 1996a,b), and 3β/17β-HSDH (Oppermann *et al.*, 1997). Ser158 is close to the residues Cys160 and Cys172, providing possible additional proton sources. The conserved cysteine residues are in the reduced state in all analysed crystals, independent of the presence of dithiothreitol. Conformational changes by substrate-binding as seen in a so-called substrate-binding loop in the structure of 7α-HSDH (Tanaka *et al.*, 1996b), which aligns with the mSR region Asn205 to Asp229 (helices αFG1 and αFG2), do not occur in mSR. This part seems rather rigid with temperature factors below 20 $Å^2$ in mSR.

As confirmed by several complex structures, the active site is highly accessible in the crystals of SR by opening the substrate-binding pockets towards honeycomb-like cavities. Major structural changes induced on binding of active site ligands are not observed.

Coenzyme-binding mode

The MIR-phased electron density already clearly identified the functional cofactor binding site of the enzyme. The adenine moiety of NADP is bound sandwiched between the side chains of Arg43, Leu71 and Leu127, and is anchored via hydrogen bonds to Asp70 and Leu71. On the basis of the first crystal structure at very high resolution of an NAD(P) co-factor in the enzyme-bound state, we are able to determine not only the conformation of the co-factor with high precision, but also the stereochemistry for the optimal hydride transfer reaction. The bound NADP molecule is in an extended conformation with the adenine ring in *anti* and the nicotinamide ring in *syn* conformation (Figure 4C), quite similar to the structures of HSDH and DHPR. The distance between C6 of the adenine and C2 of the nicotinamide is 14.2 Å for mSR, which is close to the values of 14.4 Å for 7α-HSDH, 14.6 Å for 3α,20β-HSDH and 15.1 Å for DHPR (Tanaka *et al.*, 1996b). The *syn* conformation for the nicotinamide ring allows a B-face hydride transfer reaction. Both ribose rings have a C^2-endo puckering. The distances between Tyr171 OH and the carbonyl oxygen atom and between the C-4 of the nicotinamide and the carbonyl carbon atom are 2.7 Å and 3.2 Å, respectively. The stacking interaction of Arg43 with the adenine ring stabilizes the position of this residue similar to glutathione reductase reported by Pai *et al.* (1988). Arg43 is conserved in all known members of the SDR family which prefer NADP(H) (Tanaka *et al.*, 1996a) instead of NAD(H).

Catalytic mechanism

SR catalyses the NADPH-dependent reduction of various monocarbonyl compounds including ketones and aldehydes. SR is capable of catalysing the NADPH-dependent reduction of both side-chain keto groups of 6-pyruvoyl tetrahydropterin (PH_4) to produce BH_4 with proper stereochemistry (Katoh and Sueoka, 1984; Smith, 1987). Asp258 seems essential in determining the substrate binding specificity and anchors pterin derivatives for the reduction at their monoketo or diketo side chains.

Mouse SR represents the first member of the SDR family in complex with a substrate and a product. Thus, the complex structures of SR set the stage for the detailed scenario of the catalytic reaction. The catalytic mechanism of SR appears to consist of a stereospecific transfer of a hydride ion from the exposed C-4 of the nicotinamide to the carbon of the carbonyl group of the substrate and abstraction of a proton from Tyr171 by the incipient negatively charged carbonyl oxygen. Lys175 stabilizes the position and orientation of the nicotinamide nucleoside moiety of the bound cofactor NADP through a bifurcated hydrogen bond to both the 2′-hydroxyl and 3′-hydroxyl group of the ribose group comparable with carbonyl reductase reported by Tanaka *et al.* (1996a). After side chain motion, Lys175 is able to stabilize the position of the hydroxyl group of the tyrosine base catalyst by concomitantly lowering its pK_a.

A common mechanism within the SDR family was suggested to involve a tyrosine and a lysine residue, both conserved within short-chain dehydrogenases/reductases (Jörnvall *et al.*, 1981; Ghosh *et al.*, 1994).

The first isolated intermediate in the reduction of PH_4 by SR is 1′-hydroxy-2′-oxo tetrahydropterin (Smith, 1987); this is also the compound produced in the reverse reaction from BH_4 (Curtius *et al.*, 1985). These data indicate that the enzyme preferentially reduces the 1′ keto group, consistent with the high reactivity of the enzyme toward sepiapterin and lactoyl tetrahydropterin as compared with 1′-hydroxy-2′-oxo tetrahydropterin. There are two possible pathways for complete reduction of the diketo substrate. First, after reduction of the C1′ carbonyl function and side-chain reorientation towards Tyr171 OH and NADPH C4′N, caused by the change in hybridization of the C1′ carbon atom, the second reduction step could take place at the C2′ carbonyl function. The second, stereochemically more attractive, alternative is that the reduction only occurs at the C1′ carbon atom and the second carbonyl function is reduced after isomerization at the C1′ and C2′ via an enediol intermediate which is stereospecifically stabilized by the Tyr171 anion. Evidence for an enediol form of sepiapterin was obtained by NMR studies (Iwanami and Akino, 1975). This isomerization is also catalysed in the absence of NADPH in the conversions of 6-lactoyl H_4 pterin and 6-lactoyl 7,8-BH_2 (sepiapterin) into the 6-1′-hydroxy-2′-oxopropyl pterins (Katoh and Sueoka, 1987). The tetrahydro isomers were observed as the monoketo intermediates in the *de novo* BH_4 biosynthesis (Smith, 1987). There are other examples of isomerization of a keto-hydroxy group before reduction to the diol: reduction of camphoroquinone by 3α-HSDH (Boutin, 1986) and in the reduction of cortisol to cortol in corticosteroid metabolism (Monder and Bradlow, 1980). Thus, the initial step of the conversion of PH_4 to BH_4 is the NADPH-dependent reduction at the side-chain C1′-keto function conducive to the formation of 1′-OH-2′-oxopropyl PH_4 (Figure 5; reaction 1). Internal rearrangement of

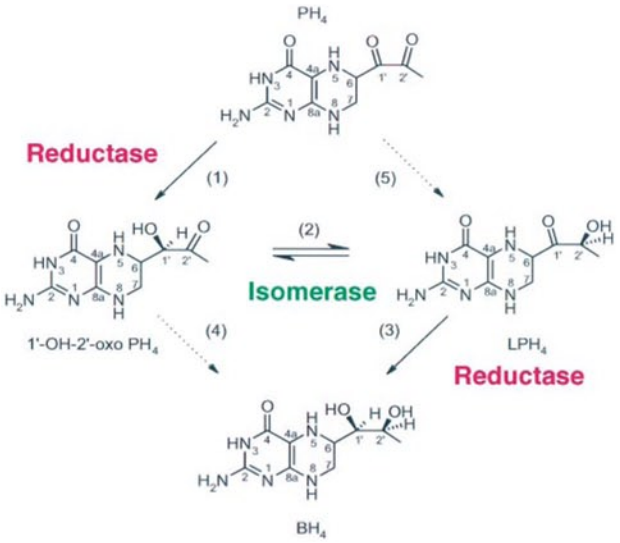

Fig. 5. Catalysed reaction of SR: reductase and isomerase. SR catalyses the sequential diketo reduction of PH_4 (6-pyruvoyl tetrahydropterin) conducive to the formation of BH_4 via an essential isomerization step of the mono-keto intermediates (reactions 1–3). For C2′-reduction of the 2′-mono keto intermediate (reaction 4), an essential reorientation of the substrate's side chain toward Tyr171 and NADPH can be proposed. The reduction of the 2′-oxo function of PH_4 (reaction 5) is presumably not catalysed by SR.

the keto group via side chain isomerization forms the 1′-keto compound LPH_4 (6-lactoyl tetrahydropterin) (Figure 5; reaction 2). Finally, this intermediate is reduced to BH_4 in an NADPH-dependent step (reaction 3). Because of an unfavourable stereochemistry at the C1′-carbonyl atom of PH_4, the alternative reduction of PH_4 first at the 2′-oxo function is presumably not catalysed by SR (reaction 5). However, reduction at the 1′-position (reaction 1) could reorientate the side-chain C2′-carbonyl towards Tyr171 and NADPH, enabling at least a less favoured reduction at the 2′-oxo function toward BH_4 (reaction 4).

The binding pockets for substrate and cofactor are opening to opposite sides of the molecule. Thus, the oxidized cofactor may be exchanged after the first reduction step for a second equivalent of NADPH while the substrate remains bound. The kinetic mechanism of the SR reaction is then proposed as an ordered bi-bi mechanism (Sueoka and Katoh, 1982).

Inhibition of SR

Competitive inhibition of SR seems feasible for pterin- and non-pterin substrates. Anchoring of an analogue to Asp258 inhibits the reduction and isomerization of pterin derivatives, whereby the catalysis of small non-pterin substrates remains possible. However, binding of an inhibitor, like oxaloacetate, directly to the catalytic centres of the active site, Tyr171 and NADP C4′N, disables the enzyme for both pterin- and non-pterin substrates (Figure 4D).

Katoh *et al.* (1982) reported that *N*-acetyl serotonin (NAS) is a potent inhibitor of partially purified rat brain and homogeneous rat erythrocyte SR (K_i = 0.2 and 0.17 μM, respectively). These data suggested that NAS binds at the substrate site and Smith *et al.* (1992) proposed the *N*-acetyl group and indole hydroxyl function of NAS critical for binding. The binding mode of NAS is shown in Figure 6, derived from a 2.1 Å refined complex structure of mSR with NAS. The high specificity of SR for this inhibitor is achieved by anchoring the indoleamine with its hydroxyl function to Asp258 like the substrate and with its *N*-acetyl function to Tyr165 via a π-electron interaction. The presumed role of the aromatic ring is also indicated by a reorientation of the Tyr side chain after NAS binding. A sequence comparison shows a corresponding Phe residue in the enzymes from rat and human origin. Furthermore, anchoring via the substrate *N*-acetyl function explains the strongly reduced K_i value with regard to serotonin. The inhibitor NAS is bound with its indole moiety to the hydrophobic bottom of the pterin binding

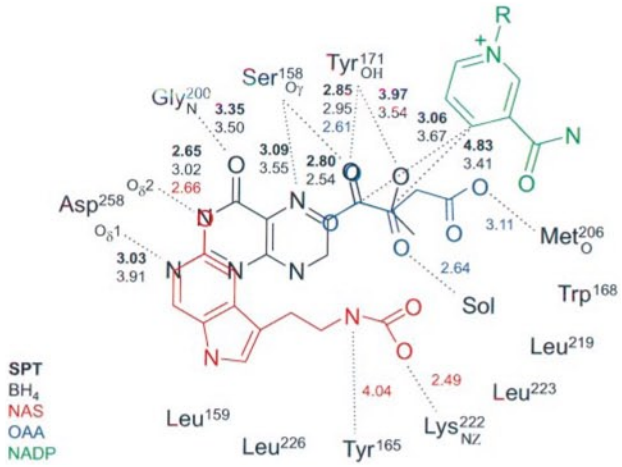

Fig. 6. Different inhibition modes for pterin- and non-pterin carbonyl substrates. The quaternary complex with NADP (nicotinamide moiety; green) shows the potent inhibitor and natural neurotransmitter *N*-acetyl serotonin NAS (red) bound with its indole moiety to Asp258. Compared with the complex structures with substrate sepiapterin (SPT) or product tetrahydrobiopterin (BH_4) (sepiapterin shown in black, hydrogen bond distances for sepiapterin shown in bold), the hydroxyl function of NAS is imitating the N3-nitrogen of the natural substrate. The inhibitor oxaloacetate OAA (blue) is imitating with its α-keto terminal carboxylate group the C1′-carbonyl function of the substrate's side chain. Hydrogen bonds are indicated by broken lines and the corresponding distances (Å) are shown according to the colour coding of the ligands.

site formed by Leu159, Leu226 and Tyr260, and with its acetyl group into a hydrophobic side pocket of the active site formed by the side chains of the residues Tyr165, Trp168, Leu219 and Leu223. Thereby, the phenyl ring of NAS binds in the pyrimidine pocket of the enzyme with its 5-hydroxyl aligned at the pyrimidine 3-position. The same binding mode can be proposed for melatonin, however, with a sterically less favourable methoxy group replacing the hydroxyl position of NAS.

In summary, SR evaluates two very specific binding motifs for competitive inhibition of the enzyme (versus sepiapterin): the Asp258 anchor, embedded in a hydrophobic pterin binding site, and Tyr165, forming a nitrogen anchor within a hydrophobic side pocket of the active site close to Asp258 and Tyr171. *In vivo*, only NAS seems to be optimally able to occupy both of these two motifs by forming a strong inhibitory complex with SR (K_i = 0.12 μM). Neither serotonin (K_i = 2.3 mM), an intermediate in the indoleamine pathway just before NAS and lacking the *N*-acetyl group, nor melatonin (K_i = 30 μM), directly after NAS with an additional methoxy group at the aromatic hydroxyl position of NAS, can achieve this tight binding mode. Because the acetyl group of NAS is not completely filling the hydrophobic pocket around Tyr165, elongation of the inhibitor's side chain should increase the binding ability. This is realized in the case of synthetic inhibitors, like *N*-chloro- or *N*-methoxy-acetyl serotonin, which are one of the tightest inhibitors known so far (K_i value = 0.006 μM, respectively 0.008 μM). Based on the crystal structure of the ternary complex with NAS and OAA, it should be possible to design synthetic inhibitors, which bind to three specific sites within the active site of SR, namely Asp258, the hydrophobic pocket near Tyr165, and Tyr171.

Oxaloacetate is already bound to native crystals of the recombinant protein expressed in *E.coli* and was crystallographically identified. Its α-keto terminal carboxylate group bound to Tyr171 imitates the C1′-carbonyl function of the substrate side chain. The inhibitory role of oxaloacetate requires further investigations by kinetic studies. Oxaloacetate can be replaced by soaking the protein with sepiapterin. It is remarkable that malate dehydrogenase (MDH), which catalyses the regeneration of oxaloacetate in the final reaction step of the citric acid cycle, shows significant overall structural homology with SR.

In order to confirm the binding mode of NAS to the active site also without OAA, the latter was removed from the protein using sepiapterin and charcoal before crystallization. The analysed ternary complex structure of the enzyme with NAS and NADP exactly confirmed the binding mode found in the quaternary complex with NAS, OAA and NADP.

Comparison with other structures

SDR members and other single-domain oxidoreductases. More than 50 different enzymes have been characterized as belonging to the SDR family (Jörnvall *et al.*, 1995). In contrast, the three-dimensional structures have been elucidated only for four enzymes of this family: 3α,20β-hydroxysteroid dehydrogenase (3α,20β-HSDH) (Ghosh *et al.*, 1994), dihydropteridine reductase (DHPR) (Varughese *et al.*, 1992), 7α- hydroxysteroid dehydrogenase (7α-HSDH) (Tanaka *et al.*, 1996b), and mouse lung carbonyl reductase (MLCR) (Tanaka *et al.*, 1996a). Despite the fact that the amino acid sequence identity among these enzymes is <30%, they share a similar tertiary structure with SR. SR, DHPR (122 Cα atoms aligning within 3.0 Å with mSR) and 17β-HSDH (159 Cα atoms) are dimeric enzymes, while MLCR (183 Cα atoms), 7α-HSDH (174 Cα atoms) and 3α,20β-HSDH (171 Cα atoms) are tetrameric. The recently solved crystal structure of the isoniazid target of *Mycobacterium tuberculosis* (enoyl-acyl carrier protein reductase; InhA) (Dessen *et al.*, 1995), shows a single-domain oxidoreductase not belonging to the SDR family, however, revealing 146 Cα atoms aligning to mSR.

The three enzymes of the pathway of BH_4 biosynthesis. The topology of the structure of SR is different from the first two enzymes of the BH_4 pathway, which show a similar subunit fold by comparing the C-terminal domain of CYH with PTPS (Nar *et al.*, 1995b). The most striking difference between SR and the former two enzymes in the pathway is a parallel β-sheet of SR instead of the anti-parallel, barrel-forming β-sheets of CYH and PTPS. However, SR shows the same architecture as CYH and PTPS with regard to a β-sheet flanked by the two helices αB and αG (mSR). The complex structures of the three enzymes with their natural substrates establish a common binding motif for pterins quite similar to the GTP binding motif in small GTP binding proteins (Bourne *et al.*, 1991). Despite the varying nature of the three substrates, which are subsequently processed in the BH_4 biosynthetic pathway (Figure 1), the guanidino function is specifically recognized by the active sites of the three enzymes by either a Glu or Asp residue. The affinity between carboxylic acids and the 2-amino pyrimidine moiety has been demonstrated in several studies (Etter and Adsmond, 1990). The residues Glu152 (*E.coli* CYH), Glu107 (rat liver PTPS), and Asp258 (mSR), respectively, form hydrogen bonds with both of its carboxylate oxygens to the substrate nitrogens N-2 and N-3. Supporting this anchor, a preceding peptide bond between Val150 and Gln151 in CYH, Thr105 and Thr106 in PTPS, or Ser158 and Leu159 in SR, forms a hydrogen bond with its amide hydrogen to the C-4 oxo group of the purine. There is no sequence identity among the three enzymes.

Significance and implications

According to the kinetic results, almost all of the activity of brain or erythrocyte SR is inhibited by NAS or melatonin. Both indoleamines are synthesized in the pineal gland via the rate-limiting and BH_4-dependent step catalysed by tryptophan hydroxylase. The role of melatonin in circadian rhythm generation, seasonal cycles and sleep has been extensively described (Brown, 1994; Morgan and Mercer, 1994). Because serotonin synthesis is regulated by modulating the rate of conversion of L-tryptophan to 5-hydroxytryptophan (Boadle-Biber, 1993), there is evidence that BH_4 participates in the short-term control of 5-hydroxytryptophan synthesis. Controlling serotonin levels in the appropriate regions of the brain has an obvious therapeutic benefit because of multiple effects of this compound with regard to tranquilizers, hallucinogens and antidepressants. In contrast to tyrosine hydroxylase,

Table I. Data collection and refinement statistics

Data set	Resolution (Å)	Total/unique reflections	Completeness (%), overall/outer shell	R_s[a]	Binding sites[b]	Phasing power[c]
NAT1	1.25	630 228/112 800	99.6/97.3	6.8	–	–
NAT2	1.95	316 626/31 613	99.8/97.8	10.9	–	–
SEP1	1.95	304 866/31 227	99.7/96.4	9.9	–	–
NAS2	2.10	167 681/23 193	93.2/88.4	6.1	–	–
BH4	2.60	49 237/12 941	95.3/87.4	12.7	–	–
NAA1	2.30	128 806/19 115	98.3/93.6	9.6	–	–
ADR3	2.50	113 085/18 884	98.1/94.8	11.0	–	–
HGAC	2.00	94 996/25 696	88.7/57.0	16.3	7	2.15
TABR	1.80	183 153/35 977	95.3/65.3	11.2	2	0.94
UONO	2.20	114 934/21 314	94.0/89.4	7.4	4	0.55

Data set	Complex ligands	Atoms	Solvent molecules	R_{cryst}/R_{free}[d]	Average *B*-factor (Å^2)	R.m.s. deviations[e], bonds (Å)/angles(°)
NAT1	OAA,NADP	3894	484	20.0/22.2	29.0	0.007/1.581
NAT2	OAA,NADP	1972	–	24.7/28.4	29.1	0.008/1.924
SEP1	SPT,NADP	2456	419	17.6/21.6	24.8	0.009/1.729
NAS2	NAS,OAA,NADP	2480	412	16.6/20.2	20.5	0.008/1.738
BH4	BH4,NADPH	2456	415	17.2/24.9	26.3	0.010/1.930
NAA1	NAS,NADP	2456	415	18.8/23.5	21.2	0.008/1.823
ADR3	ADR/NADP	2456	415	20.5/26.1	25.9	0.010/1.850

NAT1, NAT2: native crystals, containing OAA and NADP; SEP1: soak with 10 mM sepiapterin (SPT); NAS2: soak with 5 mM NAS; BH4: soak with NADPH and 10 mM BH_4; NAA1: soak with 10 mM NAS, using protein without bound OAA; ADR3: protein without bound OAA, co-crystallized with 10 mM noradrenaline; HGAC: soak with 1 mM $Hg(OAc)_2$; TABR: soak with 5 mM Ta_6Br_{14}; UONO: soak with 1 mM $UO_2(NO_3)_2$.
[a]R_{merge}: $R_s = \Sigma(I-\langle I\rangle)/\Sigma(I)$, where I is the measured intensity and $\langle I\rangle$ is the averaged value; the summation is over all measurements.
[b]Heavy atom binding sites.
[c]Phasing power, F_H/residual: r.m.s. mean heavy atom contribution/rms residual, defined as $[(F_{PHcalc}{}^2-F_{PH}{}^2)/N]^{1/2}$ with the sum over all reflections, where F_{PHcalc} is the calculated structure factor and F_{PH} is the structure factor amplitude of the heavy atom contribution, respectively.
[d]Free *R* factor, calculated by setting aside 5% of the reflections before refinement.
[e]R.m.s. deviations from ideal values.

tryptophan hydroxylase is not subject to inhibition by the end product of the reaction pathway (Joh *et al.*, 1975). Since in the brain the level of the pteridine co-factor is relatively low and may be limiting, rapid modulation of tryptophan monooxygenase activity could occur *in vivo* by small changes of an available pool of BH_4 to control the regulation of the biosyntheses of serotonin in brain (Kaufman, 1975). The specific and strong inhibitory complex between SR and NAS gives evidence for a feedback regulatory mechanism between the formation of BH_4 and indoleamines *in vivo*. Additionally, the complex with noradrenaline raises the possibility of a similar mechanism controlling the biosynthesis of catecholamines at the reaction step of SR.

Furthermore, the exceptionally high resolution of the crystal structure of SR may facilitate rational drug design also for other single-domain oxidoreductases, such as the HSDHs, implicated in controlling blood pressure or in breast cancer, or the non-SDR oxidoreductase InhA, a drug-target of *Mycobacterium tuberculosis* for AIDS patients, who develop tuberculosis.

Materials and methods

Cloning

The native cDNA sequence coding for the murine SR was adapted to the codon usage of highly expressed proteins of *E.coli* (Grantham *et al.*, 1981) and cloned in the expression vector p602/-CAT (Mörtl *et al.*, 1996), yielding the plasmid p602–SRP13. The *E.coli* M15[pGB3] host strain (Stüber *et al.*, 1990), carrying the pGB3 repressor plasmid for the overexpression of the lac repressor protein, was transformed with the plasmid. In this strain the cDNA is under control of the T5 promotor and the lac operator.

Overexpression and purification

A culture of recombinant *E.coli* was grown in Terrific Broth medium (Sambrook *et al.*, 1989) containing 150 mg/l ampicillin and 20 mg/l kanamycin. In the late logarithmic phase the culture was induced by addition of isopropyl-β-D-galactopyranoside to a final concentration of 2 mM and was harvested at 18–24 h after induction. The cells were centrifuged (5000 r.p.m., 10 min, 4°C), washed with 0.9% NaCl, re-centrifuged and resuspended in 5 ml of buffer A (10 mM MES, 2.5 mM EDTA, 1 mM DTT, 0.02% NaN_3, pH 6.5) per 1 g of wet cells. Bacteria were lysed by ultrasonic treatment, and the cellular debris was removed by centrifugation (15 000 r.p.m., 20 min, 4°C). The supernatant was loaded on a Matrix Red A Sepharose column equilibrated with buffer A. The column was washed successively with 4 vols of buffer A, 1 vol. of buffer A containing 0.5 mM NADH and 3 vols of buffer A. The protein was eluted with 1 vol. of buffer A containing 0.5 mM NADP and 1 vol. of buffer A. The enzymatic activity of SR was monitored as described previously (Ferre and Naylor, 1988; Kerler *et al.*, 1990). Fractions were constantly cooled to 0°C. The pH of the solution was adjusted to pH 8 by the addition of 10 mM NaOH and kept constant during the slow addition of solid $(NH_4)_2SO_4$ to a final concentration of 1.5 M. After 30 min the precipitated protein was harvested by centrifugation (15 000 r.p.m., 20 min, 4°C). The supernatant was applied to a Butyl–Sepharose column equilibrated with buffer B [10 mM MES, 2.5 mM EDTA, 0.02% NaN_3, 1 mM DTT, 1.5 M $(NH_4)_2SO_4$, pH 8.0]. After washing the column with 2 vols of buffer B, the protein was eluted with a linear gradient [1.5–0 M $(NH_4)_2SO_4$] over 15 vols. Fractions were monitored by enzyme assay and SDS–PAGE. Fractions showing a single protein band were combined and dialysed against 10 mM MES, pH 6.5. The solution was centrifuged for 20 h at 55 000 r.p.m., 4°C. The supernatant was removed and the colourless protein pellet was dissolved overnight at 4°C.

Crystallization

Crystallization experiments were performed at 4°C employing the vapour diffusion technique. Crystals from mSR protein (5.5 mg/ml protein

concentration), buffered in 20 mM MES, pH 6.5, 1 mM DTT, 10 mM NADP, appeared within 12 days using 1.5 M ammonium sulfate, buffered with 0.1 M citrate to pH 4.7, and grew within 3 weeks to a size of 400 μm×600 μm. The crystals are hexagonal bipyramids and belong to the space group $P6_522$ with lattice constants of $a = b = 116.86$ Å, $c = 104.78$ Å, $\gamma = 120°$. The asymmetric unit contains one molecule SR as determined by volume measurement and quantitative amino acid analysis of three crystals of different volume (Kiefersauer *et al.*, 1996). The crystals have a solvent content of 66% ($V_m = 3.66$ Å^3/Da) and diffract to a resolution of 1.2 Å. The crystal packing is honeycomb-like with the walls formed by protein. The hexagonal c-axis is centred in each comb with a diameter of 75 Å, which explains the significant anisotropy of the temperature factors especially in the direction of the c-axis, as described later.

Data collection and soaking conditions

Data sets to 1.9 Å resolution were collected with a Mar Research imaging plate system installed on a Rigaku rotating anode generator by taking 1.0° frames for at least 30° around the c-axis. Native diffraction data to a resolution of 1.22 Å were collected from a cryofreezed crystal at the BW6 beamline at DESY (Hamburg) ($\lambda = 1.0$ Å, 0.5° frames). Under cryo conditions the cell constants were reduced to $a = b = 115.88$ Å and $c = 103.78$ Å. The crystals were mounted into a fibre loop, which was prepared in a pulled-out microinjection capillary. The glass capillary was fixed into a magnetic basis for fast mounting on a goniometer head. The crystals were flash-cooled in a 95 K nitrogen beam in the presence of 25% glycerol as cryoprotectant. Data from heavy atom derivatives were obtained at 16°C by soaking crystals at 4°C either for 3 h in a solution containing 1 mM $Hg(OAc)_2$, for 1 day in 5 mM Ta_6Br_{14}, or for 3 h in 1 mM $UO_2(NO_3)_2$. The complex structure with the substrate sepiapterin was obtained by soaking crystals for 30 min in a solution containing 10 mM sepiapterin. The crystals coloured yellow during soaking with sepiapterin and maintained this colour during the entire data collection period. The complex with the product BH_4 was prepared after 15 min preincubation of the crystals with reduced NADPH by soaking for 30 min with a solution of 10 mM BH_4. The enzyme was complexed with NAS by soaking crystals for 30 min with a solution of 5 mM NAS.

Recombinantly expressed protein already contained oxaloacetate bound to the active site. Soaking crystals of oxaloacetate-containing protein with NAS led to the formation of a quaternary complex of SR with NAS, OAA and NADP. In order to analyse the crystal structure of a ternary complex of the enzyme with NAS, but without OAA, the enzyme was incubated overnight with 100 μM sepiapterin for replacing OAA from the active site, and then treated with charcoal for re-removing the sepiapterin. The protein was crystallized and soaked under the same conditions as mentioned above. The same protein, treated with sepiapterin and charcoal, was used for co-crystallization with 10 mM noradrenaline.

Data processing and phasing

All data were evaluated with MOSFLM (Leslie, 1991) and CCP4 (1994). A total of 112 800 unique reflections (630 228 total measurements) was collected for the native data set, representing 99.6% of the possible data to a resolution of 1.25 Å. The data are 99.9% complete to 1.28 Å resolution and 97.3% in the 1.28–1.25 Å shell. The R_{merge} on intensities is 6.8%. Initially, we tried to solve the structure of mSR by molecular replacement techniques. The structure of 3α,20β-HSDH (Ghosh *et al.*, 1994) with a sequence identity of 24% was used as a search model. Because this attempt failed, multiple isomorphous replacement was used for phase determination by locating heavy atom sites from isomorphous difference Patterson functions and confirming them by cross-difference Fourier syntheses. MIR phases to 2.5 Å from three derivatives [$Hg(OAc)_2$, Ta_6Br_{14}, $UO_2(NO_3)_2$] were refined using the programs PROTEIN (Steigemann, 1974) and MLPHARE (CCP4, 1994) resulting in an overall figure of merit of 0.61 (20–3.0 Å) (Table I). The space group $P6_522$ was distinguished from its enantiomorph $P6_122$ with a consistent set of heavy atom sites after inclusion of anomalous dispersion data.

Model building and refinement

Model building was done with FRODO and O (Jones *et al.*, 1990) and refinement with X-PLOR (Engh and Huber, 1991; Brünger, 1992). After solvent flattening with DM (Cowtan and Main, 1996) almost the complete model could be built into the density. The initial model built gave an *R*-factor of 40.5% ($R_{free} = 46.8\%$) after refinement with X-PLOR using the native data set NAT2. After one round of model building and combination of model and experimental phases using SIGMAA (Read, 1986), the complete model comprising 261 amino acids had been placed in the density and the *R*-factor had decreased after refinement to 24.7 Å ($R_{free} = 28.4\%$; data from 8.0 to 2.0 Å). No solvent molecules have been placed into the 2.0 Å electron density (NAT2). By increasing the resolution stepwise, the model was refined to 1.25 Å using the native data set NAT1. At a resolution of 1.4 Å and an *R*-factor of 24.7% ($R_{free} = 27.7\%$) all polar hydrogens were included and the F_{obs} were scaled to the F_{calc} by using overall anisotropic *B*-factor refinement by means of X-PLOR resulting in a direction-dependent correction for the vibration ellipsoid of –2.362 Å^2 along the axes a^* and b^* (B_{11}, B_{22}) and –5.661 Å^2 along c^* axis (B_{33}). The current model, refined to 1.25 Å, comprises 2436 C, N, O atoms, and 1410 hydrogen atoms. 484 solvent molecules have been placed solely into a well-defined F_o–F_c electron density contoured at 3 σ and in a $2F_o$–F_c electron density contoured at 1 σ. Two ions of sulfate are bound to the residues Arg220 and Arg79, the latter in close proximity to the co-factor-binding residue, Arg43. Finally, alternative conformations were refined for six side chains. The crystallographic *R*-factor of the model is 20.0% for all unique reflections from 8.0–1.25 Å resolution ($R_{free} = 22.2\%$). The r.m.s. deviations from ideal stereochemistry are 0.007 Å for bond lengths and 1.581° for bond angles (Engh and Huber, 1991). The stereochemistry of the model was verified using the program PROCHECK (Laskowski *et al.*, 1993). The dihedral angles of the polypeptide backbone all lie in allowed regions of the Ramachandran diagram. The model refined to 1.25 Å resolution was used as an apo model for refinement of all other complex structures after rigid body refinement by means of X-PLOR. The ligands were built into the resulting difference electron density and were included for final refinement. Ribbon representations of the main-chain folding of the molecule were drawn using the programs MOLSCRIPT (Kraulis, 1991) and RENDER (Merritt and Murphy, 1994). The coordinates have been deposited with the Protein Data Bank Brookhaven, NY, under accession numbers 1SEP and IOAA.

Acknowledgements

We thank Dr Herbert Nar and Tarmo Ploom for helpful discussions and critically reading the manuscript. Dr Hans D.Bartunik is gratefully acknowledged for expert assistance during crystallographic data collection at the BW6 beamline at DESY (Hamburg). This work was supported by the EC grant ERBCHRXCT 930243 (pteridines: biosynthesis, regulation and pharmacology), the Deutsche Forschungsgemeinschaft and the Fonds der Chemischen Industrie.

References

Auerbach,G. and Nar,H. (1997) The pathway from GTP to tetrahydrobiopterin: three-dimensional structures of GTP cyclohydrolase I and 6-pyruvoyl tetrahydropterin synthase. *Biol. Chem.*, **378**, 185–192.

Boadle-Biber,M.C. (1993) Regulation of serotonin synthesis. *Prog. Biophys. Mol. Biol.*, **60**, 1–15.

Bourne,H.P., Sanders,D.A. and McCormick,F. (1991) The GTPase superfamily: conserved structure and molecular mechanism. *Nature*, **349**, 117–127.

Boutin,J.A. (1986) Camphorquinone reduction: another reaction catalyzed by rat liver cytosol 3α-hydroxysteroid dehydrogenase. *Biochim. Biophys. Acta*, **870**, 463–472.

Brown,G.M. (1994) Light, melatonin and the sleep–wake cycle. *J. Psychiatry Neurosci.*, **19**, 345–353.

Brünger,A.T. (1992) *X-PLOR, Version 3.1: A System for Crystallography and NMR*. Yale University Press, New Haven, CT.

Bürgisser,D.M., Thöny,B., Redweik,U., Hess,D., Heizmann,C.W., Huber,R. and Nar,H. (1995) 6-pyruvoyl tetrahydropterin synthase, an enzyme with a novel type of active site involving both zinc binding and an intersubunit catalytic triad motif. *J. Mol. Biol.*, **253**, 358–369.

Citron,B.A., Milstien,S., Gutierrez,J.C., Levine,R.A., Yanak,B.L. and Kaufman,S. (1990) Isolation and expression of rat liver sepiapterin reductase complementary DNA. *Proc. Natl Acad. Sci. USA*, **16**, 6436–6440.

Collaborative Computational Project, Number 4 (1994) The CCP4 suite: programs for protein crystallography. *Acta Crystallogr.*, **D50**, 760–763.

Cowtan,K. and Main,P. (1996) Phase combination and cross validation in iterated density-modification calculation. *Acta Crystallogr.*, **D52**, 43–48.

Curtius,H.-C., Niederwieser,A., Levine,R.A., Lovenberg,B., Woggon,B. and Angst,J. (1983) Successful treatment of depression with tetrahydrobiopterin. *Lancet*, **1**, 657–658.

Curtius,H.-C., Heintel,D., Ghisla,S., Kuster,T.H., Leimbacher,W. and Niederwieser,A. (1985) Biosynthesis of tetrahydrobiopterin in man. *J. Inher. Metab. Dis. Suppl.*, **1**, 28–33.

Dessen,A., Quemard,A., Blanchard,J.S., Jacobs,W.R.,Jr and Sacchettini,J.C. (1995) Crystal structure and function of the isoniazid target of *Mycobacterium tuberculosis*. *Science*, **267**, 1638–1641.

Endrizzi,J.E., Cronk,J.D., Wang,W., Crabtree,G.R. and Alber,T.A. (1995) Crystal structure of DCoH, a bifunctional, protein-binding transcriptional coactivator. *Science*, **268**, 556–559.

Engh,R.A. and Huber,R. (1991) Accurate bond and angle parameters for X-ray protein structure and refinement. *Acta Crystallogr.*, **A47**, 392.

Etter,M.C. and Adsmond,D.A. (1990) The use of cocrystallization as a method of studying hydrogen bond preferences of 2-aminopyrimidine. *J. Chem. Soc. Chem. Commun.*, **8**, 589–591.

Ferre,J. and Naylor,E.W. (1988) Sepiapterin reductase in human amniotic and skin fibroblasts chorionic villi and various blood fractions. *Clin. Chim. Acta*, **271**, 271–282.

Ficner,R., Sauer,U.H., Stier,G. and Suck,D. (1995) Three-dimensional structure of the bifunctional protein PCD/DCoH, a cytoplasmic enzyme interacting with transcription factor HNF1. *EMBO J.*, **14**, 2034–2042.

Ghosh,D., Wawrzak,Z., Weeks,C.M., Duax,W.L. and Erman,M. (1994) The refined three-dimensional structure of 3α,20β-hydroxysteroid dehydrogenase and possible roles of the residues conserved in short-chain dehydrogenases. *Structure*, **2**, 629–640.

Grantham,R., Gautier,M., Gouy,M., Jacobzone,M. and Mercier,R. (1981) Codon catalog usage is a genome strategy modulated for gene expressivity. *Nucleic Acids Res.*, **9**, 43–74.

Hemmens,B. and Mayer,B. (1996) Enzymology of nitric oxide synthases. In Titheradge,M.A. (ed.), *Methods in Molecular Biology, Vol. 100, Nitric Oxide Protocols*. Humana Press, Totowa, NJ, pp. 1–32.

Ichinose,H., Katoh,S., Sueoka,T., Titani,K., Fujita,K. and Nagatsu,T. (1991) Cloning and sequencing of complementary DNA encoding human sepiapterin reductase: an enzyme involved in tetrahydrobiopterin biosynthesis. *Biochem. Biophys. Res. Commun.*, **179**, 183–189.

Iwanami,Y. and Akino,M. (1975) Evidence for the enediol form of sepiapterin. *J. Nutr. Sci. Vitaminol.*, **21**, 143–145.

Joh,T.H., Shikimi,T., Pickel,V.M. and Reis,D.J. (1975) Brain tryptophan hydroxylase: purification of, production of antibodies to, and cellular and ultrastructural localization in serotonergic neurons of rat midbrain. *Proc. Natl Acad. Sci. USA*, **72**, 3575–3579.

Jones,T.A., Bergdoll,M. and Kjeldgaard,M. (1990) O: a macromolecule modelling environment. In Bugg,C. and Ealick,S. (eds), *Crystallography and Modelling Methods in Molecular Design*. Springer-Verlag, New York, pp. 189–199.

Jörnvall,H., Persson,M. and Jeffery,J. (1981) Alcohol and polyol dehydrogenases are both divided into two protein types, and structural properties cross-relate the different enzyme activities within each type. *Proc. Natl Acad. Sci. USA*, **78**, 4226–4230.

Jörnvall,H., Persson,B., Krook,M., Atrian,S., Gonzalez-Duarte,R., Jeffery,J. and Ghosh,D. (1995) Short-chain dehydrogenases/reductases (SDR). *Biochemistry*, **34**, 6003–6013.

Katoh,S., Sueoka,T. and Yamada,S. (1982) Direct inhibition of brain sepiapterin reductase by a catecholamine and an indoleamine. *Biochem. Biophys. Res. Commun.*, **105**, 75–81.

Katoh,S. and Sueoka,T. (1984) Sepiapterin reductase exhibits a NADPH-dependent dicarbonyl reductase activity. *Biochem. Biophys. Res. Commun.*, **118**, 859–866.

Katoh,S. and Sueoka,T. (1987) Isomerization of 6-lactoyl tetrahydropterin by sepiapterin reductase. *J. Biochem.*, **101**, 275–278.

Kaufman,S. (1975) In Mandell,A.J. (ed.), *Neurobiological Mechanisms of Adaptation and Behavior*. Raven Press, New York, pp. 127–136.

Kerler,F., Ziegler,I., Schmid,C. and Bacher,A. (1990) Synthesis of tetrahydrobiopterin in friend erythroleukemia cells and its modulator effect on cell proliferation. *Exp. Cell. Res.*, **189**, 151–156.

Kiefersauer,R., Stetefeld,J., Gomis-Rüth,F.X., Romao,M.J., Lottspeich,F. and Huber,R. (1996) Protein-crystal density by volume measurement and amino-acid analysis. *J. Appl. Crystallogr.*, **29**, 311–317.

Kraulis,P.J. (1991) MOLSCRIPT: a program to produce both detailed and schematic plots of protein structures. *J. Appl. Crystallogr.*, **24**, 946–950.

Laffranchi,R., Schoedon,G., Blau,N. and Spinas,G.A. (1997) Tetrahydrobiopterin synthesis precedes nitric oxide-dependent inhibition of insulin-secretion in INS-1 rat pancreatic β-cells. *Biochem. Biophys. Res. Commun.*, **233**, 66–70.

Laskowski,R.A., MacArthur,M.W., Moss,D.S. and Thornton,J.M. (1993) PROCHECK: a program to check the stereochemical quality of protein structures. *J. Appl. Crystallogr.*, **26**, 283–291.

Leslie,A.G.W. (1991) Macromolecular data processing. In Moras,D., Podjarny,A.D. and Thierry,J.C. (eds), *Crystallographic Computing V*. Oxford University Press, Oxford, pp. 27–38.

Lovenberg,W., Levine,R.A., Robinson,D.S., Ebert,M., Williams,A.C. and Calne,D.B. (1979) Hydroxylase cofactor activity in cerebrospinal fluid of normal subjects and patients with Parkinson's disease. *Science*, **204**, 624–626.

Lowenstein,J. and Snyder,S.H. (1992) Nitric oxide, a novel biologic messenger. *Cell*, **70**, 705–707.

Marletta,M.A. (1994) Nitric oxide synthase: aspects concerning structure and catalysis. *Cell*, **78**, 927–930.

Mataga,N., Imamura,K. and Watanabe,Y. (1991) 6R-tetrahydrobiopterin perfusion enhances dopamine, serotonin, and glutamate outputs in dialysate from rat striatum and frontal cortex. *Brain Res.*, **551**, 64–71.

McGeer,P.J., Eccles,J.C. and McGeer,E.G. (1987) In *Molecular Neurobiology of the Mammalian Brain*. 2nd edn. Plenum Press, New York, pp. 319–346.

Merritt,E.A. and Murphy,M.E.P. (1994) Raster3D version 2.0. A program for photorealistic molecular graphics. *Acta Crystallogr.*, **D50**, 869–873.

Milstien,S. and Kaufman,S. (1989) Immunological studies on the participation of 6-pyruvoyl tetrahydropterin (2′-oxo) reductase, an aldose reductase, in tetrahydrobiopterin biosynthesis. *Biochem. Biophys. Res. Commun.*, **165**, 854–860.

Monder,C. and Bradlow,H.L. (1980) In Greep,R.O. (ed.), *Recent Progress in Hormone Research. Vol. 36.* Academic Press, New York, pp. 345–400.

Morgan,P.J. and Mercer,J.G. (1994) Control of seasonality by melatonin. *Proc. Nutr. Soc.*, **53**, 483–493.

Mörtl,S., Fischer,M., Richter,G., Tack,J., Weinkauf,S. and Bacher,A. (1996) Biosynthesis of riboflavin: lumazine synthase of *Escherichia coli*. *J. Biol. Chem.*, **271**, 33201–33207.

Nar,H., Huber,R., Heizmann,C.W., Thöny,B. and Bürgisser,D.B. (1994) Three-dimensional structure of 6-pyruvoyl tetrahydropterin synthase, an enzyme involved in tetrahydrobiopterin biosynthesis. *EMBO J.*, **13**, 1255–1262.

Nar,H. *et al*. (1995a) Active site topology and reaction mechanism of GTP cyclohydrolase I. *Proc. Natl Acad. Sci. USA*, **92**, 12120–12125.

Nar,H., Huber,R., Meining,W., Schmid,C., Weinkauf,S. and Bacher,A. (1995b) Atomic structure of GTP cyclohydrolase I. *Structure*, **3**, 459–466.

Nichol,C.A., Lee,C.L., Edelstein,M.P., Chao,J.Y. and Duch,D.S. (1983) Biosynthesis of tetrahydrobiopterin by *de novo* and salvage pathways in adrenal medulla extracts, mammalian cell cultures, and rat brain *in vivo*. *Proc. Natl Acad. Sci. USA*, **80**, 1546–1550.

Oppermann,U.C.T., Filling,C., Berndt,K.D., Persson,B., Benach,J., Ladenstein,R. and Jörnvall,H. (1997) Active site directed mutagenesis of 3β/17β-hydroxysteroid dehydrogenase establishes differential effects on short-chain dehydrogenase/reductase reactions. *Biochemistry*, **36**, 34–40.

Ota,A., Ichinose,H. and Nagatsu,T. (1995) Mouse sepiapterin reductase: an enzyme involved in the final step of tetrahydrobiopterin biosynthesis. Primary structure deduced from the cDNA sequence. *Biochim. Biophys. Acta*, **1260**, 320–322.

Pai,E.F., Karplus,P.A. and Schulz,G.E. (1988) Crystallographic analysis of the binding of NADPH, NADPH fragments, and NADPH analogues to gluthathione reductase. *Biochemistry*, **27**, 4465–4474.

Pfleger,R.C., Piantadosi,C. and Snyder,F. (1967) The biocleavage of isomeric glyceryl ethers by soluble liver enzymes in a variety of species. *Biochim. Biophys. Acta*, **144**, 633–648.

Read,R.J. (1986) Improved coefficients for map calculation using partial structures with errors. *Acta Crystallogr.*, **A42**, 140–149.

Rossmann,M.G., Liljas,A., Bränden,C.-I. and Banaszak,L.J. (1975) Evolutionary and structural relationships among dehydrogenases. In Boyer,P.D. (ed.), *The Enzymes.* Academic Press, New York, pp. 61–102.

Sambrook,J., Fritsch,E.F. and Maniatis,T. (1989) *Molecular Cloning: A Laboratory Manual*. Cold Spring Harbor Laboratory Press, Cold Spring Harbor, NY.

Schallreuter,K.U., Wood,J.M., Pittelkow,M.R., Gütlich,M., Lemke,K.R., Rodl,W., Swanson,N.N., Hitzemann,K. and Ziegler,I. (1994) Regulation of melanin biosynthesis in the human epidermis by tetrahydrobiopterin. *Science*, **263**, 1444–1446.

Smith,G.K. (1987) On the role of sepiapterin reductase in the biosynthesis of tetrahydrobiopterin. *Arch. Biochem. Biophys.*, **255**, 254–266.

Smith,G.K. and Nichol,C.A. (1984) Two new tetrahydropterin intermediates in the adrenal medullary de novo biosynthesis of tetrahydrobiopterin. *Biochem. Biophys. Res. Commun.*, **120**, 761–766.
Smith,G.K., Duch,D.S., Edelstein,M.P. and Bigham,E.C. (1992) New inhibitors of sepiapterin reductase. *J. Biol. Chem.*, **267**, 5599–5607.
Steigemann,W. (1974) *Die Entwicklung und Anwendung von Rechenverfahren und Rechenprogrammen zur Strukturanalyse von Proteinen*. PhD Thesis, Technische Universität München, Germany.
Stüber,D., Matile,H. and Garotta,G. (1990) In *Immunological Methods, Vol. 4*. Academic Press, Orlando, FL, pp. 121–152.
Sueoka,T. and Katoh,S. (1982) Purification and characterization of sepiapterin reductase from rat erythrocytes. *Biochim. Biophys. Acta*, **717**, 265–271.
Tanaka,K., Kaufman,S. and Milstien,S. (1989) Tetrahydrobiopterin, the cofactor for aromatic amino acid hydroxylases, is synthesized by and regulates proliferation of erythroid cell. *Proc. Natl Acad. Sci. USA*, **86**, 5864–5867.
Tanaka,N., Nonaka,T., Nakanashi,M., Deyashiki,Y., Hara,A. and Mitsui,Y. (1996a) Crystal structure of the ternary complex of mouse lung carbonyl reductase at 1.8 Å resolution: the structural origin of coenzyme specificity in the short-chain dehydrogenase/reductase family. *Structure*, **15**, 33–45.
Tanaka,N., Nonaka,T., Tanabe,T., Yoshimoto,T., Tsuru,D. and Mitsui,Y. (1996b) Crystal structures of the binary and ternary complexes of 7 α-hydroxysteroid dehydrogenase from *Escherichia coli*. *Biochemistry*, **35**, 7715–7730.
Varughese,K.I., Skinner,M.M., Whiteley,J.M., Matthews,D.A. and Xuong,N.H. (1992) Crystal structure of rat liver dihydropteridine reductase. *Proc. Natl Acad. Sci. USA*, **89**, 6080–6084.

Received on July 24, 1997; revised on August 18, 1997